Deep-sea observations and modeling of the 2004 Sumatra tsunami in Drake Passage

Alexander B. Rabinovich,[1,2] Philip L. Woodworth,[3] and Vasily V. Titov[4]

Received 28 May 2011; revised 7 July 2011; accepted 7 July 2011; published 23 August 2011.

[1] The 2004 Sumatra tsunami was clearly recorded by two UK bottom pressure gauges, DPN and DPS, deployed in Drake Passage between South America and Antarctica. These open-ocean records were examined to estimate characteristics of the tsunami waves and to compare the results of numerical simulations with the observations. Maximum wave heights measured at these gauges were 4.9 cm at DPN and 7.4 cm at DPS; the travel times from the source area were 19 h 46 min and 19 h 39 min respectively, consistent with the times obtained from the nearby coastal tide gauges. The numerical model described well the frequency content, amplitudes and general structure of the observed waves, with only small time shifts probably related to wave dispersion effects. The shifts were 15 min for DPN and 10 min for DPS, with the modeled waves leading the observations in each case. Further inspection of the simulated and observed records revealed that the identified tsunami waves are related to the second (main) train of waves propagating by the energy conserving route along the mid-ocean ridges, while the first train of waves travelling by the fastest route across the ocean remained unrecognizable in the observed DPS and DPN records and undetectable in the records of coastal tide gauges because of their insignificant amplitudes compared to the background variability. **Citation:** Rabinovich, A. B., P. L. Woodworth, and V. V. Titov (2011), Deep-sea observations and modeling of the 2004 Sumatra tsunami in Drake Passage, *Geophys. Res. Lett.*, *38*, L16604, doi:10.1029/2011GL048305.

1. Introduction

[2] The M_w = 9.3 Sumatra megathrust earthquake (estimated as 9.1 by the USGS) of 00:59 UTC 26 December 2004 produced highly destructive tsunami waves that severely damaged the coastal regions in the Indian Ocean and killed more than 230,000 people [*Bernard and Robinson*, 2009]. The 2004 Sumatra tsunami was the first global tsunami to occur during the "instrumental era", and it was clearly recorded by a large number of tide gauges throughout the World Ocean [cf. *Merrifield et al.*, 2005; *Woodworth et al.*, 2005; *Rabinovich and Thomson*, 2007; *Candella et al.*, 2008]. Global tsunami propagation models demonstrate that mid-ocean ridges served as wave-guides to the 2004 event [cf. *Titov et al.*, 2005; *Kowalik et al.*, 2007], efficiently transmitting tsunami energy from the source area near northwestern Sumatra to far-field regions of the World Ocean [*Rabinovich et al.*, 2006]. The Indian Ocean tsunami waves moved south-eastward around Australia and New Zealand into the Pacific Ocean and south-westward around South Africa into the Atlantic Ocean. These semi-global propagating "Pacific" and "Atlantic" waves met in the area of Drake Passage between Tierra del Fuego and the Antarctic Peninsula (Figure 1), making this a region of specific interest.

[3] Fortunately, two Bottom Pressure Recorders (BPRs) of the Proudman Oceanographic Laboratory (POL, now called the National Oceanography Centre, Liverpool) were deployed in Drake Passage during the 2004 event (Figure 1). These instruments clearly recorded the arriving tsunami waves, providing unique open-ocean *in situ* information on the far-field characteristics of the waves, converging from the Atlantic and the Pacific. These deep-sea records enabled us to examine the "pure" characteristics of the 2004 Sumatra waves (undistorted by coastal effects), compare them with the information obtained from the nearby mainland and island coastal tide gauges and provide a validation of the global MOST (Method Of Splitting Tsunami) model [*Titov and González*, 1997; *Titov et al.*, 2005] in this remote region of high scientific importance and complexity.

2. Observations

[4] POL has a long history of using BPRs, primarily for tidal and ocean circulation studies [cf. *Spencer and Vassie*, 1997]. During December 2004, POL had two BPRs deployed in the South Indian Ocean (IO1 and IO2) [*Rietbroek et al.*, 2006] and two in Drake Passage (DPN and DPS) (Figure 1); these instruments are believed to have been among the very few bottom pressure gauges working during the 2004 event and the only open-ocean instruments in the southern oceans. The northern and southern Drake Passage recorders were deployed at approximately 1090 m depth for the purpose of continuing the monitoring of Antarctic Circumpolar Current variability now spanning two decades [cf. *Woodworth et al.*, 2006]; the pressure and temperature data from these two recorders can be obtained from www.pol.ac.uk/ntslf/acclaimdata/bprs/.

[5] The Atlantic Ocean historically has had until recently no Tsunami Warning System and no standard instruments designed for tsunami measurements. Two coastal United Kingdom (UK) tide gauges were operational in the region of Drake Passage at nearby islands: Port Stanley (Falkland Is.) and Signy (South Orkney Is.) (Figure 1). However, because the primary purpose of these tide gauges, as well as the DPN and DPS BPRs, was the measurement of relatively low-frequency processes (tides, storm surges, seasonal and climatic sea level variations) [cf. *Woodworth et al.*, 2005], all these gauges had a relatively long sampling (averaging)

[1]Institute of Ocean Sciences, Department of Fisheries and Oceans, Sidney, British Columbia, Canada.
[2]P.P. Shirshov Institute of Oceanology, Russian Academy of Sciences, Moscow, Russia.
[3]National Oceanography Centre, Liverpool, UK.
[4]Pacific Marine Environmental Laboratory, NOAA, Seattle, Washington, USA.

0094-8276/11/2011GL048305

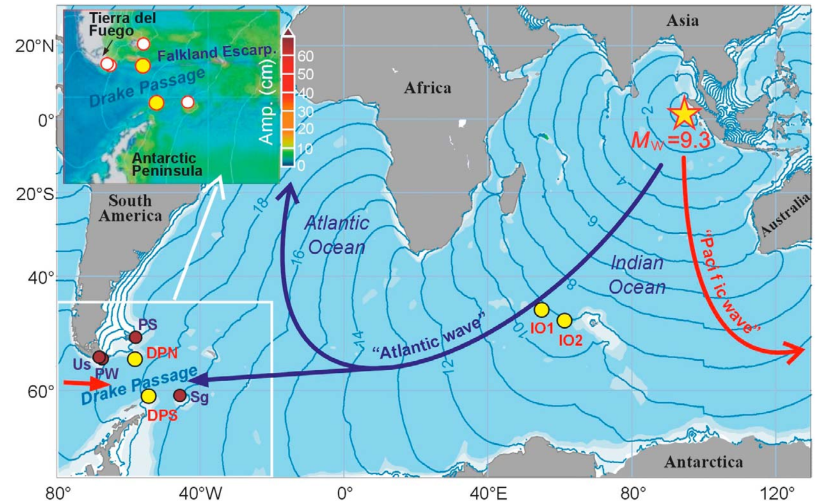

Figure 1. Propagation of the 2004 Sumatra tsunami waves from the source area (yellow star) into the Drake Passage region (white box); a dark blue curved arrow indicates the "Atlantic wave", a red arrow indicates the "Pacific wave". Yellow circles mark bottom pressure recorders IO1, IO2, DPN and DPS; brown (white in the insert) circles mark coastal tide gauges Signy, South Orkney Is (Sg), Port Stanley, Falkland Is (PS), Puerto Williams, Chile (PW) and Ushuaia, Argentina (Us). The small insert shows simulated tsunami wave heights for the region from *Titov et al.* [2005] along with the locations of certain topographic features.

interval of $\Delta t = 15$ min. Nevertheless, the instruments clearly recorded the 2004 tsunami waves (Figure 2). For comparison, we used two coastal gauges located in the narrow Beagle Channel in the southern part of Tierra del Fuego: Ushuaia, Argentina, and Puerto Williams, Chile (Figure 1), which had sampling intervals of $\Delta t = 6$ min and 2 min, respectively. Both gauges clearly recorded the 2004 Sumatra tsunami [*Candella et al.*, 2008]. Principal parameters of the recorded tsunami waves at these six stations are shown in Table 1.

[6] According to the observations, the tsunami waves first arrived at Signy (about 17.8 h after the earthquake); then approximately two hours later at deep-sea stations DPN and DPS; then two hours later again at Port Stanley and Puerto Williams; and finally at Ushuaia (at 22.1 h after the earthquake). The estimated parameters were consistent and in good agreement with each other. The first wave at all stations was positive, supporting the notion that the frontal crest wave propagated westward and southwestward from the source area, while the first trough wave went eastward [cf. *Titov et al.*, 2005; *Rabinovich and Thomson*, 2007]. The observed period at all stations was about 45 min, with the only exception Port Stanley (60 min). The trough-to-peak wave heights, except at the sheltered station of Ushuaia, were also quite similar (44–52 cm) which is 7–10 times greater than at the deep-ocean stations DPN and DPS (4.9–7.4 cm). A significant increase of the tsunami signal at coastal stations, in comparison with open-ocean stations, is related to the topographic amplification of the incoming tsunami waves on the shelf and in local bays and inlets. The open ocean tsunami records uncontaminated by coastal effects make them especially valuable for comparison with the results of numerical modeling.

3. Numerical Simulation

[7] To examine and interpret tsunami waves in the region of Drake Passage we used the global tsunami MOST model of *Titov et al.* [2005]. Snapshots of simulated waves in Figure 3 illustrate different stages of the 2004 Sumatra tsunami entering the region. The "Atlantic wave", travelling from the ESE and with the positive (crest) wave moving in front, was the first to arrive (Figure 3a). The "Pacific wave" arrived from the west about three hours later (Figures 3b and 3c). However, it was mainly reflected by cross-passage bottom fractures and turned to the north along the coast of Chile (Figure 3d). The Atlantic wave interacted with the island chains and was scattered by strong coastal and bottom irregularities, in particular by the Falkland Escarpment (see insert in Figure 1), leading to rather complicated cellular wave structure in this region (Figure 3d). A most encouraging fact is that, despite the complicated structure of the tsunami waves in the region of Drake Passage, the observed oscillations at stations DPN and DPS were consistent with the simulated records (Figure 4). This appears to have been the first time when model results could be verified with the use of open-ocean observations from such remote sites (~11,000 km from the source area).

[8] Comparing simulated and observed tsunami records, we found that the former were 10 min ahead of the DPS

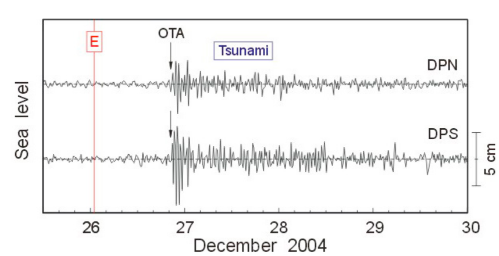

Figure 2. Tsunami records from bottom stations DPN and DPS in Drake Passage. The solid vertical red line labeled "E" indicates the time of the main earthquake shock; arrows denote the observed tsunami arrival time (OTA) of the first wave.

Table 1. Tsunami Characteristics Estimated From Bottom Pressure and Coastal Tide Gauge Records in and Near Drake Passage

Station	Country	Coordinates	Sampling Interval (min)	First Wave: Sign, Arrival Time (UTC)	First Wave: Travel Time	Maximum Wave Height (cm)	Period (min)
Signy, Orkney Is.	UK	60.72°S; 45.60°W	15	(+) 18:45	17 h 46 m	52	45
DPN	UK	54.94°S; 58.36°W	15	(+) 20:45	19 h 46 m	4.9	45
DPS	UK	60.85°S; 54.71°W	15	(+) 20.38	19 h 39 m	7.4	45
Port Stanley, Falkland Is.	UK	51.75°S; 57.93°W	15	(+) 22:30	21 h 31 m	44	60
Puerto Williams	Chile	54.56°S; 67.37°W	2	(+) 22:42	21 h 43 m	47	44
Ushuaia	Argentina	54.49°S; 68.22°W	6	(+) 23:12	22 h 13 m	20	45

record and 15 min ahead of the DPN record; the differences were less than 1.3% of the propagation time. The structure of the tsunami waveforms was not distorted and after incorporating these small shifts, the computed wave trains perfectly coincided in phase with the observed ones (Figure 4). In general, the simulated results are affected by the errors in the model bathymetry and wave dispersion. The MOST model is based on a non-dispersive shallow-water approximation [*Titov and Synolakis*, 1997; *Titov and González*, 1997]. While the wave dispersion effects may be expected to influence the tsunami wave trains at such large propagation distances, we do not see much discrepancy between the measured and modeled waves. Partly this can be explained by the low-frequency nature of the 2004 tsunami (due to the enormous extent of the 2004 Sumatra source region: about 1200–1300 km according to *Stein and Okal* [2005]), which would result in only small dispersion effects, and partly because the MOST model exhibits numerical dispersion that mimics the dispersive equations fairly well [*Burwell et al.*, 2007] (see also *Shuto* [1991] for a detailed discussion of this problem). The application of this model for several recent events in the Pacific Ocean, where many deep-ocean records were available for comparison, indicated that for such low-frequency events the numerical dispersion substitutes reasonably well for the actual wave dispersion [*Wei et al.*, 2008].

[9] The results of the numerical modeling reproduce accurately the main frequencies and the general structure of the observed waves at the DPN and DPS sites, in particular the stronger and more regular oscillations at the southern site compared with the northern site. It is difficult to directly compare the wave amplitudes of simulated and observed waves since the former records had a sampling interval of 1 min and the latter records of 15 min (average). To overcome this problem, we averaged and resampled the simulated records with 15-min average values. The resampled 15-min amplitudes are about 35% smaller than the original 1-min simulated amplitudes and match closely the observed amplitudes (Figure 4).

[10] Further comparison of the simulated and observed records revealed an interesting feature of the tsunami oscillations in the region of Drake Passage. According to the results of the numerical modeling, the first train of tsunami oscillations arrived at this region at 18:47 UTC at the DPS site and at 19:33 UTC at the DPN site, i.e., 17 h 48 m and

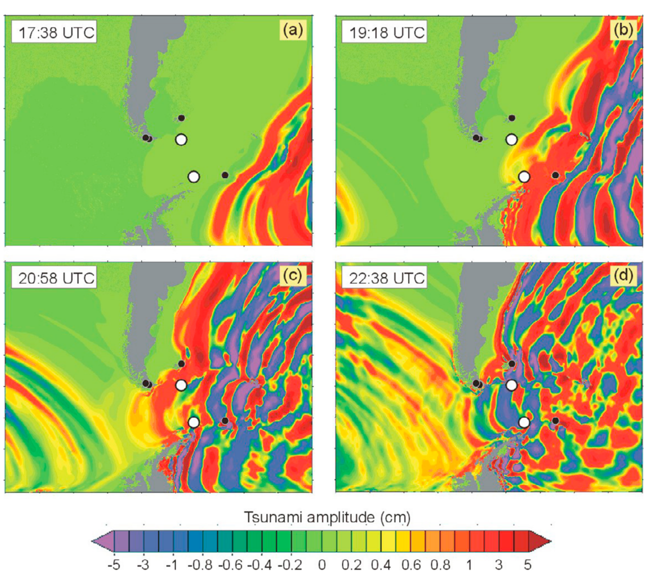

Figure 3. Snapshots of the numerically simulated 2004 tsunami waves in the region of Drake Passage. The labels indicate the times (a) 17:38, (b) 19:18, (c) 20:58, and (d) 22:38 UTC on December 26, 2004. White circles mark the locations of bottom pressure recorders DPN and DPS and black circles the locations of coastal tide gauges.

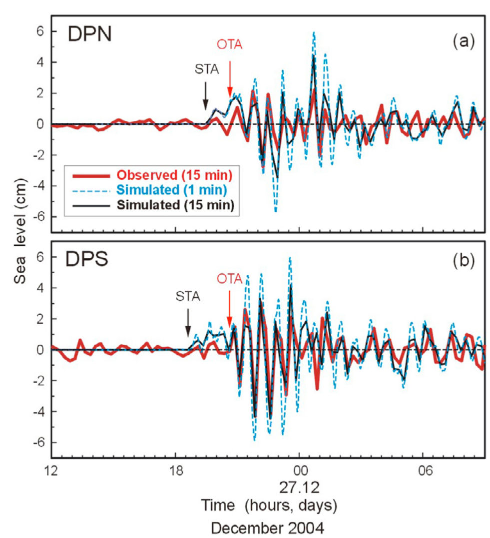

Figure 4. Numerically simulated (dashed blue line with 1-min sampling and solid black line with 15-min sampling) and observed with 15-min sampling tsunami records for (a) DPN and (b) DPS stations. For best fitting the data, the simulated records are shifted by 15 min (DPN) and 10 min (DPS). The black arrow denotes the simulated shifted tsunami arrival time (STA) of the first train of waves, which has not been identified in the observations, and the red arrow denotes the observed detected tsunami arrival (OTA).

18 h 34 m after the main shock (these are times corrected for the 10 and 15 min shifts, respectively). The "simulated tsunami arrival" times, STA (denoted in Figure 4 by arrows) are in good agreement with the "expected tsunami arrival" (ETA) times estimated by the West Coast/Alaska Tsunami Warning Center (approximately 18 h and 18 h 40 m for the areas of DPS and DPN, respectively; see http://wcatwc.arh.noaa.gov/IndianOSite/tt_atlantic.gif). However, this first train of waves is unrecognizable in the observed DPS and DPN records; it is also undetectable in the records of coastal tide gauges. What were identified as the "observed tsunami arrival" times, OTA (Table 1 and Figure 4) are the times of the main train arrival (20:38 UTC at DPS and 20:45 UTC at DPN). The result corresponds well to the 2004 Sumatra tsunami observations in the northeastern Pacific [*Rabinovich et al.*, 2006, 2011], as well as with numerical findings by *Titov et al.* [2005] and *Kowalik et al.* [2007] who demonstrated that mid-ocean ridges serve as waveguides, efficiently transmitting the tsunami wave energy by slower but more economic (energy conserving) routes. This important effect should be taken into account by the operational tsunami services. It is interesting that while the simulated times (STA) for the DPS and DPN sites are significantly different (due to the different distances for the respective fastest routes), the observed times (OTA) are quite similar indicating that the "economical" routes to the DPS and DPN sites were almost the same.

4. Discussion and Conclusions

[11] Two BPRs deployed in 2004 in Drake Passage were able to record the arrival of the Sumatra tsunami. These distant-from-source data sets have provided deep ocean observations of the tsunami frequency content, amplitude and timing, and have enabled a validation of state-of-the-art tsunami modeling. The signals seen in the two BPR data sets correspond well to the second (main) train of tsunami waves simulated by the model. These waves propagate along the energy-conserving route of the mid-ocean ridges, the amplitude of the first train waves traveling along the fastest route being too small for detection either by the BPRs or by the coastal tide gauges in the region. The importance of mid-ocean ridges as wave guides, suggested by previous studies of the Sumatra tsunami and confirmed by the present one, needs to be fully taken into account within the modeling employed by the operational tsunami warning systems. As our results show, the kinematic travel time calculations, often used for tsunami arrival time estimates without tsunami amplitude considerations, can predict significantly earlier arrival (up to several hours) than the actually observed (and often damaging) wave's arrival.

[12] The model shows a remarkable fit to the measured data in the far-field deep ocean locations, improving the confidence in using the models for predicting the ocean-wide effects of tsunamis. With the exception of the time shift, the modeled waveforms (when resampled to a lower resolution) compare very well with the records. The time shifts of 10 to 15 min of the tsunami arrival require additional investigation - enough anecdotal and published evidence has been accumulated that show such a shift to be a systematic error derived within the simulation of long distance propagation of tsunami waves over bathymetry. However the error is fairly small (~1.3%) and does not distort the rest of the modeled wave parameters, so it is fairly benign as far as models' predictive capability is concerned. In addition this error is much smaller than the potential error in the arrival time when using kinematic arrival time calculations. As far as the 15 min sampling allows, the correlation between the observed and modeled wave amplitudes and frequencies is good for several hours of the tsunami wave action. A complex structure of the modeled wave train is also close to the observations, reproducing correctly the amplitude envelope of the wave train with an increase and decay of the tsunami amplitudes during more than 12 h of wave record. It correctly shows larger wave intensity at the South (DPS) site, as compared with the North (DPN) location. This is a very stringent overall test of the model performance, since the wave have been simulated for 18 h of propagation over 11,000 km, virtually to the opposite side of the globe, before reaching the study site.

[13] The bathymetry of the Drake Passage and of the whole wave path from the source is also very challenging, with numerous island chains and ocean ridges that could serve either as wave guides or as wave scatterers. The area where the observations were made experienced an arrival of the tsunami from two opposite directions – one traveling across the Pacific Ocean and the other propagating across the Atlantic Ocean as seen in Figure 3. The temporal resolution of the measurements did not allow for a thorough analysis of these separate wave packages. However the use of the model has provided an additional means of analysis of these data. The complicated wave pattern was correctly modeled and, when compared with data, allowed for additional insight into the tsunami arrival and amplitude manifestation in the measured data. The fact that the model was not tuned at all for fitting to the data – the same source as that of *Titov et al.* [2005] was used for this study – shows promising forecast potential when using numerical models in real-time.

[14] **Acknowledgments.** The authors thank the Remote Sea Level and Instrumentation Group at the National Oceanography Centre in Liverpool for their expertise and hard work in deploying bottom pressure recorders in Drake Passage. They also thank Christopher Moore (PMEL/NOAA, Seattle, WA) for his assistance in the numerical modeling of tsunami waves.

[15] The Editor thanks Eric Geist for his assistance in evaluating this paper.

References

Bernard, E. N., and A. R. Robinson (2009), Introduction: Emergent findings and new directions in tsunami science, in The Sea, vol. 15, *Tsunamis*, edited by E. N. Bernard and A. R. Robinson, pp. 1–22, Harvard Univ. Press, Cambridge, Mass.

Burwell, D., E. Tolkova, and A. Chawla (2007), Diffusion and dispersion characterization of a numerical tsunami model, *Ocean Modell.*, *19*(1–2), 10–30, doi:10.1016/j.ocemod.2007.05.003.

Candella, R. N., A. B. Rabinovich, and R. E. Thomson (2008), The 2004 Sumatra tsunami as recorded on the Atlantic coast of South America, *Adv. Geosci.*, *14*(1), 117–128, doi:10.5194/adgeo-14-117-2008.

Kowalik, Z., W. Knight, T. Logan, and P. Whitmore (2007), The tsunami of 26 December 2004: Numerical modeling and energy considerations, *Pure Appl. Geophys.*, *164*, 379–393, doi:10.1007/s00024-006-0162-7.

Merrifield, M. A., et al. (2005), Tide gage observations of the Indian Ocean tsunami, December 26, 2004, *Geophys. Res. Lett.*, *32*, L09603, doi:10.1029/2005GL022610.

Rabinovich, A. B., and R. E. Thomson (2007), The 26 December 2004 Sumatra tsunami: Analysis of tide gauge data from the world ocean. Part 1. Indian Ocean and South Africa, *Pure Appl. Geophys.*, *164*, 261–308, doi:10.1007/s00024-006-0164-5.

Rabinovich, A. B., R. E. Thomson, and F. E. Stephenson (2006), The Sumatra tsunami of 26 December 2004 as observed in the North Pacific

and North Atlantic oceans, *Surv. Geophys.*, *27*, 647–677, doi:10.1007/s10712-006-9000-9.
Rabinovich, A. B., K. Stroker, R. E. Thomson, and E. Davis (2011), DARTs and CORK: High-resolution observations of the 2004 Sumatra tsunami in the abyssal northeast Pacific, *Geophys. Res. Lett.*, *38*, L08607, doi:10.1029/2011GL047026.
Rietbroek, R., P. LeGrand, B. Wouters, J.-M. Lemoine, G. Ramillien, and C. W. Hughes (2006), Comparison of in situ bottom pressure data with GRACE gravimetry in the Crozet-Kerguelen region, *Geophys. Res. Lett.*, *33*, L21601, doi:10.1029/2006GL027452.
Shuto, N. (1991), Numerical simulation of tsunamis—Its present and near future, *Nat. Hazards*, *4*, 171–191, doi:10.1007/BF00162786.
Spencer, R., and J. M. Vassie (1997), The evolution of deep ocean pressure measurements in the U.K., *Prog. Oceanogr.*, *40*, 423–435, doi:10.1016/S0079-6611(98)00011-1.
Stein, S., and E. A. Okal (2005), Speed and size of the Sumatra earthquake, *Nature*, *434*, 581–582, doi:10.1038/434581a.
Titov, V. V., and F. I. González (1997), Implementation and testing of the Method of Splitting Tsunami (MOST) model, NOAA *Tech. Memo. ERL PMEL-112*, Pac. Mar. Environ. Lab., NOAA, Seattle, Wash.
Titov, V. V., and C. E. Synolakis (1997), Extreme inundation flows during the Hokkaido-Nansei-Oki tsunami, *Geophys. Res. Lett.*, *24*(11), 1315–1318, doi:10.1029/97GL01128.
Titov, V. V., A. B. Rabinovich, H. Mofjeld, R. E. Thomson, and F. I. González (2005), The global reach of the 26 December 2004 Sumatra tsunami, *Science*, *309*, 2045–2048, doi:10.1126/science.1114576.
Wei, Y., et al. (2008), Real-time experimental forecast of the Peruvian tsunami of August 2007 for U.S. coastlines, *Geophys. Res. Lett.*, *35*, L04609, doi:10.1029/2007GL032250.
Woodworth, P. L., et al. (2005), Evidence for the Indonesian tsunami in British tidal records, *Weather*, *60*(9), 263–267, doi:10.1256/wea.59.05.
Woodworth, P. L., et al. (2006), Antarctic Peninsula sea levels: A real-time system for monitoring Drake Passage transport, *Antarct. Sci.*, *18*(3), 429–436, doi:10.1017/S0954102006000472.

A. B. Rabinovich, Institute of Ocean Sciences, Department of Fisheries and Oceans, 9860 West Saanich Rd., Sidney, BC V8L 4B2, Canada. (a.b.rabinovich@gmail.com)
V. V. Titov, Pacific Marine Environmental Laboratory, NOAA, 7600 Sand Point Way NE, Seattle, WA 98115-6349, USA.
P. L. Woodworth, National Oceanography Centre, 6 Brownlow St., Liverpool L3 5DA, UK.